CONSTRUCTION OF MICROFLUIDIC BIOCHIPS WITH ENHANCED FUNCTIONALITIES USING 3D FEMTOSECOND LASER DIRECT WRITING

Authors:

   Y. Cheng, Y. Liao, F. He, L. Qiao, K. Sugioka, K. Midorikawa

Corresponding author: Y. Cheng

                e-mail: ya.cheng@siom.ac.cn

Construction of microfluidic biochips with enhanced functionalities using 3D femtosecond laser direct writing

Ya Cheng[1,*], Yang Liao[1], Fei He[1], Lingling Qiao[1], Koji Sugioka[2] and Katsumi Midorikawa[2]

[1]State Key Laboratory of High Field Laser Physics, Shanghai Institute of Optics and Fine Mechanics, Chinese Academy of Sciences, P.O. Box 800-211, Shanghai 201800, China
[2]Laser Technology Laboratory, RIKEN - Advanced Science Institute, Hirosawa 2-1, Wako, Saitama 351-0198, Japan

[*]Email: ya.cheng@siom.ac.cn

Abstract

The extreme nonlinear interaction between femtosecond laser pulses and large-band-gap materials has enabled three-dimensional (3D) microfabrication inside transparent materials. In the past decade, this technique has been used for creating a variety of functional components in glass materials, including microoptics, microfluidics, microelectronics, micromechanics, etc. Using these building blocks, femtosecond laser microfabrication also allows for construction of highly integrated microdevices. Here, we provide an overview of our latest progress made along this direction, including focal spot engineering and nanofluidic fabrication. In particular, we show that 3D micro-/nano-fluidic components with arbitrary geometries can be directly formed inside glass. This opens up promising prospects for a broad spectrum of applications based on compact and complex 3D microfluidic networks. Our work shows that this technique holds promise for fabricating 3D hybrid micro-systems, such as Lab-on-a-chip devices and Micro Total Analysis Systems in the future.

Introduction

Microfluidics provides unique capabilities of controlling and manipulating tiny volumes of liquids with high precision and ease of operation, thus it has enabled downsizing of both chemical and biological analysis [1, 2]. Femtosecond laser direct writing has been employed for creating 3D hollow structures embedded in glass which serves as microfluidic elements such as microchannels and microchambers. Furthermore, femtosecond laser irradiation can alter the optical properties of glass for creating a wide range of micro-optical components inside glass [3-5]. This capability opens up new avenues for fabricating a variety of integrated optofluidic microchips for chemical sensing and biological analysis.

In this contribution, we focus on two achievements we made along this direction recently. This first is related to focal spot engineering using spatiotemporally shaped femtosecond laser pulses [6-7]; and the second is related to fabrication of micro-/nanofluidic structures with nearly arbitrary lengths and 3D geometries and configurations in porous glass [8-10].

Focal spot engineering by beam shaping

The cross sectional shape of the microchannels plays an important role for many lab-on-a-chip applications, because it determines the fluidic dynamics and biological function in the microchannel. Microfluidic channels produced using single-scan transverse writing technique, i.e., the sample is translated perpendicular to the beam propagation direction intrinsically have highly elliptical cross sections due to elongation of the focal spot in the propagation direction of the laser beam. Previously, several beam shaping techniques have been developed to overcome this problem, e. g., producing microfluidic channels of highly asymmetric cross sectional shapes. Typical shaping techniques include astigmatic beam shaping [11], slit beam shaping [12], crossed-beam shaping [13], etc. Nevertheless, the ideal solution is to realize an isotropic 3D fabrication resolution with only a single objective lens, which cannot be achieved with any of the above-mentioned shaping techniques.

Here, we offer a different solution to control the cross section by employing temporal focusing of the femtosecond laser pulses [6]. The core of this technique is to separate the spectral components of the femtosecond pulses in space before the pulses enter the objective lens. Temporal focusing occurs because the spatial overlapping of different frequency components only happens around the focus, leading to the shortest pulse duration and consequently, the highest peak intensity. This will facilitate an improved axial resolution of the femtosecond laser microfabrication because the peak intensity will decrease rapidly due to the

broadening of the pulse duration when moving away from the geometric focal spot. The details of this technique can be found in Ref. [14].
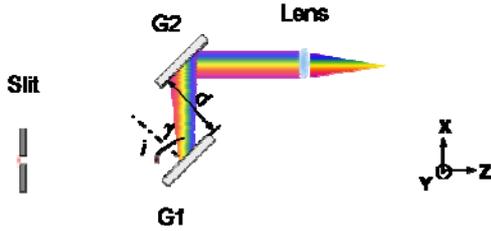

Fig. 1 Schematic of spatial-temporal focusing geometry.

Schematic of our spatial-temporal focusing geometry is shown in Fig. 1. Our chirped pulse amplification (CPA) system delivers 40 fs laser pulses at a center wavelength of 800 nm with a spectral bandwidth of ~30 nm and polarized along the Y direction. In this experiment, the input laser beam size is controlled by an adjustable circular aperture. To produce the spatially chirped incident pulses, a pair of parallel gratings (1200 line/mm, blazing at 800 nm) are used to separate the spectral components of the incident pulse in X coordinate. The distance between the gratings is set to be ~180 mm and the incident angle ~ 45° in our experiment. To pre-compensate the chirp induced by all the optics such as neutral density (ND) filters, objective lens, and the grating pair, the input pulse is positively pre-chirped by adjusting the compressor in the amplifier. The best pre-compensation of dispersion can be achieved when the strongest ionization (i. e., the brightest plasma) of the air was observed at the focus of the objective. The power of the laser pulses is adjusted by ND filters before being focused by a 20 × objective lens (NA = 0.46) into the glass sample. The PC-controlled XYZ stage has a resolution of 1 μm.

To experimentally demonstrate the control of cross-sectional aspect ratio, we fabricate 3D microchannels in fused silica by femtosecond laser direct write. In our experiment, U-shaped microchannels vertically embedded in glass are first inscribed 300 μm beneath the surface at a constant speed of 50 μm/s. In order to show that controllable cross-sectional shapes can be obtained for microchannels oriented in arbitrary directions without rotating any optical elements during the laser irradiation, we fabricate two groups of channels aligned in both X and Y directions, as illustrated in Fig. 2(a). To continuously vary the aspect ratio, the beam size and the average power of the femtosecond laser are gradually increased from 2 mm to 5 mm and from 2 mW to 4 mW, respectively. After the laser irradiation, the sample is subjected to a 150-min etching in a solution of 10% HF diluted with water in an ultrasonic bath. The microchannels are formed after all the areas modified by the femtosecond laser are completely

removed. It is noted that the group of channels oriented along X direction are formed somewhat faster than those along Y direction due to the polarization-selective etching [15].
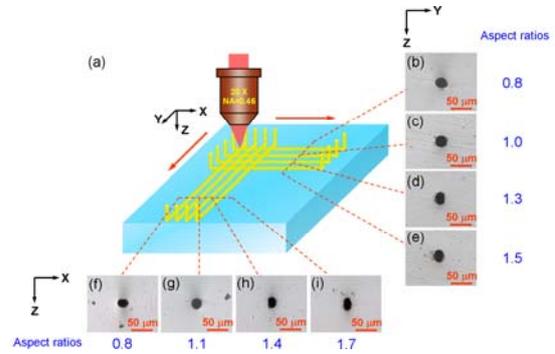

Fig. 2 (a) Schematic of the 3D microfluidic channels fabricated using the temporal focusing method. The red arrows denote the translation directions of the stage. (b)-(i) Optical micrographs of cross-section of microfluidic channels. The beam sizes and laser powers are 2 mm and 4 mW in (b), (f), 3 mm and 3.5 mW in (c), (g), 4 mm and 2 mW in (d), (h), and 5 mm and 2 mW in (e), (i).

We examine the cross sections of the channels by cutting and polishing the sample. It is found that the axial resolution of the fabrication can be continuously controlled by changing the input beam size. This is consistent with the above theoretical analysis. The aspect ratios of the cross section gradually increase from 0.8 to 1.7, as shown in Figs. 2 (b)-(i). In particular, for a laser power of 3.5 mW and a beam size of ~3 mm, the channels oriented in both X and Y directions exhibit a nearly circular cross-section, as shown in Figs. 2 (c) and (g). These results clearly suggest that a spherical focal spot with isotropic resolution in 3D space has been achieved with the temporally focused femtosecond pulses.

It should be stressed that strictly speaking, focal spot produced by temporal focusing is always slightly different from a perfect spherical spot, whereas for high-NA objective lenses, such difference is fairly insignificant. For low-NA objective lenses, one should use a combination of slit-beam shaping and temporal shaping to achieve a perfectly spherical focal spot, as we have demonstrated in Ref. [7].

Fabrication of 3D micro-/nanofluidics in porous glass

Femtosecond laser direct writing has now been widely used for producing microfluidic channels embedded in glass. Currently, there are mainly two strategies for this application. The first strategy employs femtosecond laser direct writing in either silica glass [16] or photosensitive glass [17] followed by chemical wet etching. Unfortunately, with this technique the length of the microfluidic channel that could be fabricated is limited to a few millimeters, due to the limited etch ratio between

the areas with and without the femtosecond irradiation. Another strategy is to perform femtosecond laser 3D drilling from the rear surface of the glass in contact with distilled water, by which the water introduced into the microchannel can help remove the ablated material [18]. However, when the length of the channel increases, the ablated debris can no longer be ejected from the microchannel and thus prevent the water entring into the laser affected zone (LAZ) [19]. For this reason, usually the microfluidic channels fabricated by water-assisted drilling are even shorter than those fabricated by femtosecond laser direct writing followed by chemical wet etching.
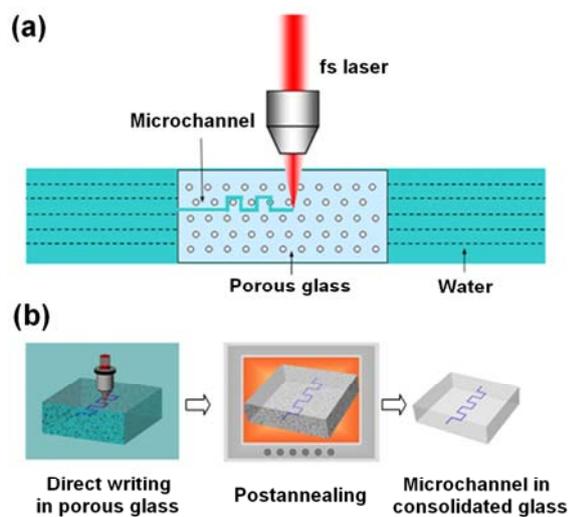

Fig. 3 (a) The schematic view of the experimental setup for water-assisted femtosecond laser direct writing inside porous glass, and (b) the flow diagram for the microchannel fabrication.

Here, we show that fabrication of long 3D microchannels with arbitrary lengths and configurations can be achieved by water-assisted femtosecond laser direct writing inside a porous glass [8]. The porous glass substrates, which has a size of 15 × 15 × 3 mm, are produced by removing the borate phase from phase-separated alkali-borosilicate glass in hot acid solution. The schematic of the water-assisted femtosecond laser direct writing inside porous glass is illustrated in Fig. 3(a). The porous glass is immersed in distilled water. The laser beam is focused into the sample, and 3D microchannels can be fabricated by moving the sample according to a preprogrammed pattern with suitable laser pulse energy, scan parameters, and focusing geometries (details will be given below). After the laser direct writing, the sample is then placed in a furnace and annealed at a temperature of 1150 °C to consolidate into a compact glass, as shown in Fig. 3(b).

A typical square-wave-like microfluidic channel as shown in Fig. 4(a) can be obtained by first performing a slow scan at a translation speed of 20 μm/s. After the slow scan, although the microfluidic channel can be formed; however, we find that some parts of the channel were blocked by debris created by laser ablation. Therefore, we further repeatedly scan the microfluidic channel 6 times at a higher translation speed of 1 mm/s in order to completely remove all the debris. After the fast scans, a through channel can be obtained as shown in Fig. 4. Figure 4(a) shows a top view micrograph of the homogeneous microchannel which has a total length of ~1.6 cm.

However, the microfluidic channel embedded in porous glass fabricated after the femtosecond laser ablation cannot be directly used for microfluidic application, because the liquid in the channel tends to permeate into the surrounding pores. In order to collapse all the pores in the porous glass, the sample is further annealed at 1150 ℃ for 1 h. Figures 4(b) and 4(c) show optical micrographs of the annealed microchannel filled with red ink. It is clear that the ink is well confined in the microchannel, which indicates that the microchannel is completely sealed because the pores have been closed after annealing. It should be specifically mentioned that after the consolidation process, the glass substrate shrinks in all the three directions by ~15%, corresponding to a volume reduction of ~39% which is in good agreement of the 40% porosity ratio of the glass. Therefore, the initial length of ~1.6 cm of the microfluidic channel decreases to ~1.4 cm after the postannealing. Moreover, the porous glass substrate, which is opaque due to the scattering of the nanopores, becomes highly transparent after the postannealing. This facilitates the future incorporation of optical functions in the glass for optofluidic applications.
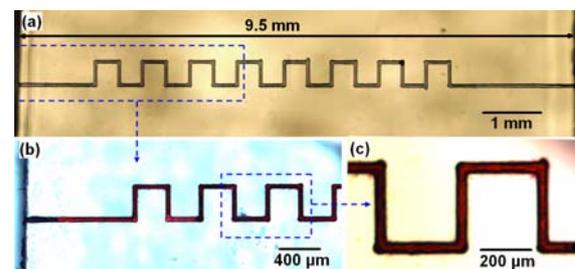

Fig. 4 (a) Top view micrograph of a 1.6-cm-long microchannel embedded in porous glass before postannealing; (b) and (c) Close-up views of postannealed microchannel filled with red ink. (b) Low magnification; (c) High magnification.

Microfluidic mixer and nanofluidics

The capability of fabrication of microfluidic channels of arbitrary lengths and 3D configurations has soon been employed for fabricating functional devices [20]. A passive micromixer based on the baker's transformation concept [21] is shown in Fig.

5. Figures 5(a) and 5(b) present the schematic illustrations of the designed 3D mixer which is composed of a Y-shape microchannel embedded 400 μm below the surface of chip and a string of mixing units, connected to two opening inlets and one outlet. Figure 3(c) present an overview of a 3D micromixer consisted of six mixing units. A close up view of the mixing unit is shown in Fig. 3(d) (top view). The length of all the horizontal and vertical channels in each mixing unit is 150 μm.
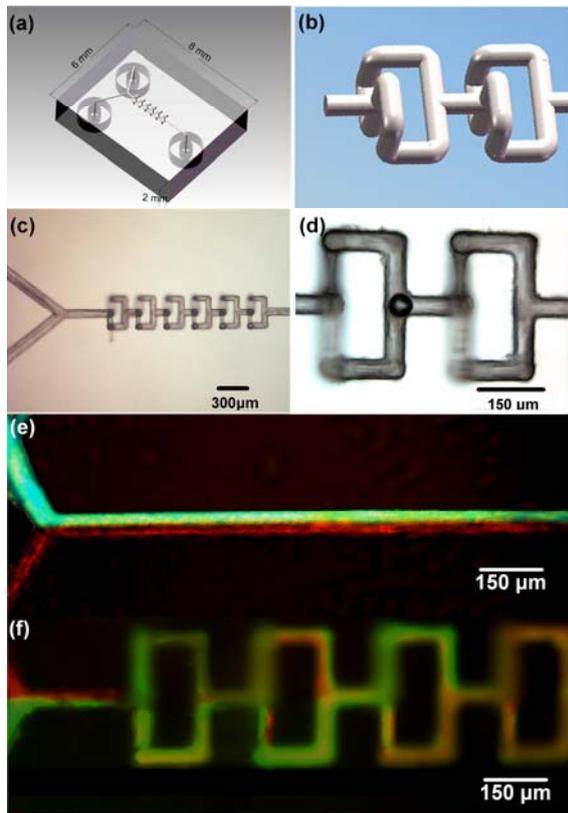

Fig. 5 Schematic diagrams of the 3D passive microfluidic mixer: (a) overview and (b) close-up view images; and optical micrographs of the fabricated 3D microfluidic mixer: (c) overview and (d) close-up view micrographs. (e) 1D and (f) 3D microfluidic mixing experiments.

Figures 5(e) and 5(f) show the experimental results of mixing of the two fluorescent dye solutions (fluorescein sodium and Rhodamine B) in the 1D and 3D microfluidic mixers fabricated under the same direct writing conditions, repectively. Clearly, the mixing behaviors in these two structures agree well with the simultion results. For the 3D mixer, after passing through three mixing units (i. e., a length of 0.9 mm), the two fluids are well mixed, corresponding to a mixing time of about 10 ms. For comparison, Fig. 5(e) shows that in the 1D microfluidic channel, efficient mixing was not achieved after a propagation distance of ~1300 μm.

Very recently, nanofluidic channels have been created inside porous glass by femtosecond laser direct writing, as shown in Figs. 6(a) and 6(b). Control of the diameter of the nanochannel is achieved by adjusting the pulse energy of the writing beam [22]. Previously, by placing the peak intensity of the femtosecond laser pulses near the ablation threshold, fabrication of nanochannels in fused silica with a resolution approaching the diffraction-limit (i. e., ~500 nm) has been achieved [23]. Here, for the first time to our knowledge, we achieve fabrication resolutions far beyond diffraction limit (i. e., ~40 nm) by combining the threshold effect and the exotic phenomenon of formation of periodic nanograting during the process of laser writing in the porous glass immersed in water. The formation of the nanograting-like structures was observed in 2003 [24] and later attributed to local field enhancement near femtosecond laser irradiation induced under-dense nanoplasmas [25]. In the porous glass, we observe that the nanograting-like structures induced by femtosecond laser irradiation constitute an array of hollow cracks with a width down to ~40 nm [22]. When the femtosecond laser intensity is intentionally reduced to a level at which only the hollow nanocrack produced in the central area of the focal volume can survive, a nanofluidic channel is produced, as shown in Fig. 6(b). The 3D nanofluidic channels open opportunities in a variety of fields of research, such as nanofluidic physics and chemistry, DNA analysis, lab on a chip, nanoplasmonics, and so forth.
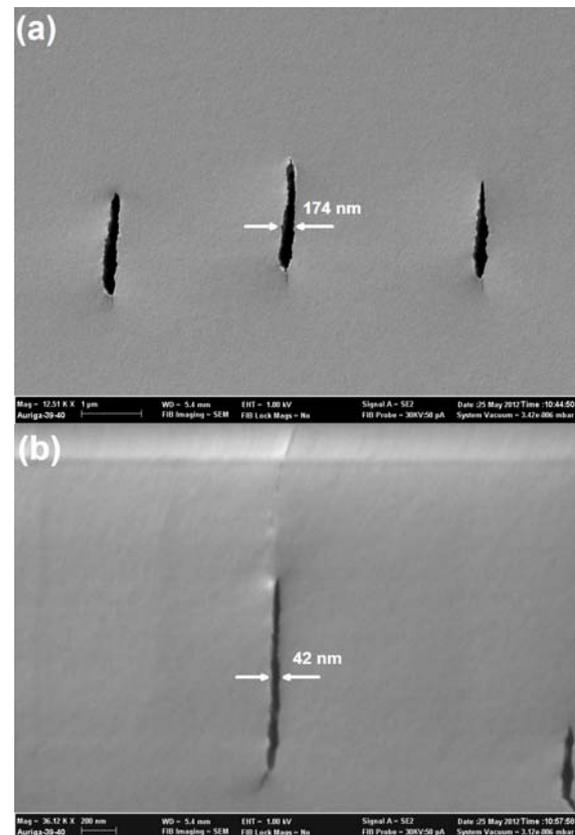

Fig. 6 Nanofluidic channels written in porous glass immersed in water using a 40 fs, 800 nm, 250 kHz femtosecond laser at different pulse energies. (a) 140 nJ/pulse; (b) 128 nJ/pulse. Writing speed: 10 μm/s; objective lens: water-immersed objective (N.A.= 1.10). Substrates have been postannealed for collapsing all the nanopores in the glass.

Conclusions

We have shown that the latest advances in femtosecond laser microprocessing have led to novel capabilities that were previously not available. In particular, we demonstrate the 3D isotropic fabrication resolution using spatiotemporally focused femtosecond laser pulses, and fabrication of 3D micro-/nanofluidics in porous glass with extreme flexibilities in terms of channel dimensions (e. g., total length, diameters, etc.) and geometries. We envision that the development of highly functional microfluidic chips and Lab-on-a-chip devices will benefited from these techniques.

References

1. A. Manz, N. Graber and H.M. Widmer (1990), Miniaturized total chemical analysis systems: A novel concept for chemical sensing, Sensor. Actuat. B, 1, 244-248.
2. G.M. Whitesides (2006), The origins and the future of microfluidics, Nature, 442, 368-373.
3. R. Osellame, H.J.W.M. Hoekstra, G. Cerullo and M. Pollnau (2011), Femtosecond laser microstructuring: an enabling tool for optofluidic lab-on-chips, Laser Photonics Rev., 5, 442-463.
4. K. Sugioka and Y. Cheng (2011), Integrated microchips for biological analysis fabricated by femtosecond laser direct writing, Mrs. Bull., 36, 1020-1027.
5. K. Sugioka and Y. Cheng (2012), Femtosecond laser processing for optofluidic fabrication, Lab Chip, 12, 3576-3589.
6. F. He, H. Xu, Y. Cheng, J. Ni, H. Xiong, Z. Xu, K. Sugioka and K. Midorikawa (2010), Fabrication of microfluidic channels with a circular cross section using spatiotemporally focused femtosecond laser pulses, Opt. Lett., 35, 1106-1108.
7. F. He, Y. Cheng, J. Lin, J. Ni, Z. Xu, K. Sugioka and K. Midorikawa (2011), Independent control of aspect ratios in the axial and lateral cross sections of a focal spot for three-dimensional femtosecond laser micromachining, New J. Phys., 13, 083014.
8. Y. Liao, Y. Ju, L. Zhang, F. He, Q. Zhang, Y. Shen, D. Chen, Y. Cheng, Z. Xu, K. Sugioka and K. Midorikawa (2010), Three-dimensional microfluidic channel with arbitrary length and configuration fabricated inside glass by femtosecond laser direct writing, Opt. Lett., 35, 3225-3227.
9. Y. Ju, Y. Liao, L. Zhang, Y. Sheng, Q. Zhang, D. Chen, Y. Cheng, Z. Xu, K. Sugioka and K. Midorikawa (2011), Fabrication of large-volume microfluidic chamber embedded in glass using three-dimensional femtosecond laser micromachining, Microfluid. Nanofluid., 11, 111-117.
10. C. Liu, Y. Liao, F. He, Y. Shen, D. Chen, Y. Cheng, Z. Xu, K. Sugioka and K. Midorikawa (2012), Fabrication of three-dimensional microfluidic channels inside glass using nanosecond laser direct writing, Opt. Express, 20, 4291-4296.
11. R. Osellame, S. Taccheo, M. Marangoni, R. Ramponi, P. Laporta, D. Polli, S.D. Silvestri and G. Cerullo (2003), Femtosecond writing of active optical waveguides with astigmatically shaped beams, J. Opt. Soc. Am. B, 20, 1559-1567.
12. Y. Cheng, K. Sugioka, K. Midorikawa, M. Masuda, K. Toyoda, M. Kawachi and K. Shihoyama (2003), Control of the cross-sectional shape of a hollow microchannel embedded in photostructurable glass by use of a femtosecond laser, Opt. Lett., 28, 55-57.
13. K. Sugioka, Y. Cheng, K. Midorikawa, F. Takase and H. Takai (2006), Femtosecond laser microprocessing with three-dimensionally isotropic spatial resolution using crossed-beam irradiation, Opt. Lett., 31, 208-210.
14. G. Zhu, J. Howe, M.E. Durst, W. Zipfel and C. Xu (2005), Simultaneous spatial and temporal focusing of femtosecond pulses, Opt. Express, 13, 2153-2159.
15. C. Hnatovsky, R.S. Taylor, E. Simova, V.R. Bhardwaj, D.M. Rayner and P.B. Corkum (2005), Polarization-selective etching in femtosecond laser-assisted microfluidic channel fabrication in fused silica, Opt. Lett., 30, 1867-1869.
16. A. Marcinkevicius, S. Juodkazis, M. Watanabe, M. Miwa, S. Matsuo, H. Misawa and J. Nishii (2001), Femtosecond laser-assisted three-dimensional microfabrication in silica, Opt. Lett., 26, 277-279.
17. K. Sugioka, Y. Cheng and K. Midorikawa (2005), Three-dimensional micromachining of glass using femtosecond laser for lab-on-a-chip device manufacture, Appl. Phys. A, 81, 1-10.
18. Y. Li, K. Itoh, W. Watanabe, K. Yamada, D. Kuroda, J. Nishii and Y.Y. Jiang (2001), Three-dimensional hole drilling of silica glass from the rear surface with femtosecond laser pulses, Opt. Lett., 26, 1912-1914.
19. D.J. Hwang, T.Y. Choi and C.P. Grigoropoulos (2004), Liquid-assisted femtosecond laser drilling of straight and three-dimensional microchannels in glass, Appl. Phys. A, 79, 605-612.
20. Y. Liao, J.X. Song, E. Li, Y. Luo, Y.L. Shen, D.P. Chen, Y. Cheng, Z.Z. Xu, K. Sugioka and K. Midorikawa (2012), Rapid prototyping of three-dimensional microfluidic mixers in glass by femtosecond laser direct writing, Lab Chip, 12, 746-749.
21. P. Carrière (2007), On a three-dimensional implementation of the baker's transformation, Phys. Fluids, 19, 118110.
22. Y. Liao, Y. Cheng, C. Liu, J. Song, F. He, Y. Shen, D. Chen, Z. Xu, Z. Fan, X. Wei, K. Sugioka and K. Midorikawa, Direct laser writing of sub-50nm nanofluidic channels buried in glass for three-dimensional micro-nanofluidic integration, submitted.
23. K. Ke, E.F. Hasselbrink and A.J. Hunt (2005), Rapidly prototyped three-dimensional nanofluidic channel networks in glass substrates, Anal. Chem., 77, 5083-5088.
24. Y. Shimotsuma, P. Kazansky, J. Qiu and K. Hirao (2003), Self-Organized Nanogratings in Glass Irradiated by Ultrashort Light Pulses, Phys. Rev. Lett., 91, 247405.
25. V.R. Bhardwaj, E. Simova, P.P. Rajeev, C. Hnatovsky, R.S. Taylor, D.M. Rayner and P.B. Corkum (2006), Optically Produced Arrays of Planar Nanostructures inside Fused Silica, Phys. Rev. Lett., 96, 057404.